OAK RIDGE NATIONAL LABORATORY
operated by
UNION CARBIDE CORPORATION
NUCLEAR DIVISION
for the
U.S. ATOMIC ENERGY COMMISSION

ORNL-TM-1839

COPY NO. - 109

DATE - June 6, 1967

Neutron Physics Division

HIGH-ENERGY NUCLEON TRANSPORT*

R. G. Alsmiller, Jr.

Abstract

In this paper the recent work on the transport of high-energy nucleons through dense matter is reviewed. The application of this transport to space-shielding studies is emphasized so the discussion is restricted to low and intermediate energies ($\leq$ 1 GeV) and to relatively thin shields.

NOTE:
This Work Supported by
NATIONAL AERONAUTICS AND SPACE ADMINISTRATION
Under Order R-104(1)

*Invited paper to be presented at the 1967 Annual Meeting of the American Nuclear Society, San Diego, California, June 11-15, 1967.

HIGH-ENERGY NUCLEON TRANSPORT*

R. G. Alsmiller, Jr.
Oak Ridge National Laboratory
Oak Ridge, Tennessee

In this paper the recent work on the transport of high-energy nucleons through dense matter is reviewed. The application of this transport to space-shielding studies is emphasized so the discussion is restricted to low and intermediate energies ($\leq$ 1 GeV) and to relatively thin shields. A review article on this subject has recently been published[1] and therefore the discussion here is, in the main, concerned with work which has become available since this review.**

The accuracy of transport calculations must be determined by comparison with experimental measurements made on thick targets, and I shall therefore begin by discussing two such comparisons that have recently been made.

J. S. Fraser et al.[2] have measured the thermal neutron flux produced when large targets of Be, Sn, Pb, and depleted uranium are bombarded by high-energy (0.5 to 2 GeV) protons. A schematic diagram of the experimental arrangement for the case of a lead target is shown in Fig. 1. In the experiment a narrow proton beam was incident on one face of a thick target which was surrounded by a large water bath, and the thermal neutron flux was measured as a function of position in the water. W. A. Coleman,[3] using the nucleon transport code written by W. E. Kinney,[4] has calculated this thermal flux for the case of 540-MeV protons on a lead target (see Fig. 1)

*Research sponsored by the National Aeronautics and Space Administration under Union Carbide Corporation's contract with the U. S. Atomic Energy Commission.

**Much of the work that will be described is unpublished. I thank all of the investigators involved for making their work available to me prior to its publication.

ORNL-DWG 66-7999

CYLINDRICAL SYMMETRY ABOUT BEAM AXIS

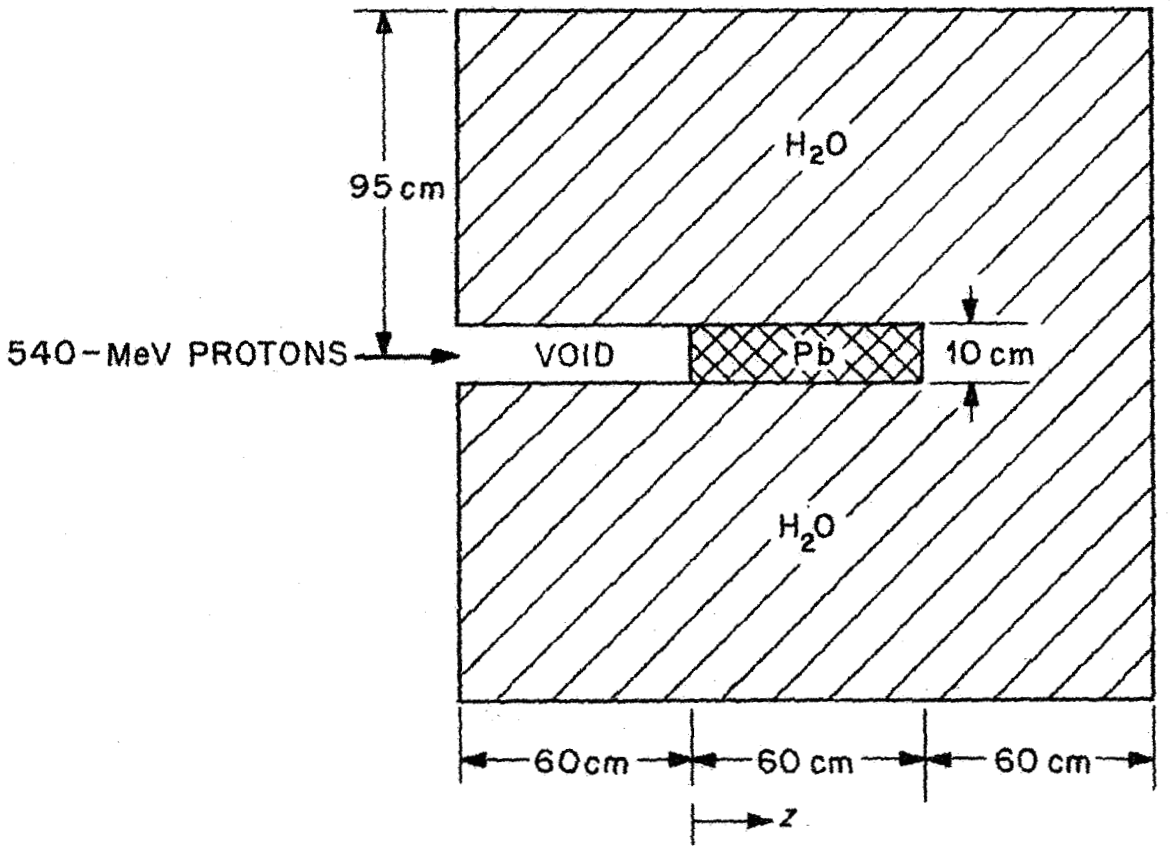

Fig. 1. ING Experiment.

and made comparisons with the experimental measurements. This transport code uses Monte Carlo methods and treats particle production from high-energy (> 50 MeV) nuclear reaction by means of an intranuclear-cascade code written by H. W. Bertini.[5] Below 50 MeV nonelastic collisions are treated by using an evaporation code written by L. Dresner,[6] and elastic collisions are treated using experimental data. In the calculations of Coleman, the geometry was the same as that shown in Fig. 1, and the thermal flux was calculated assuming a single velocity for neutrons with an energy of less than 0.5 eV.

The comparisons between the calculated and measured values are shown in Figs. 2 and 3. In the figures the thermal flux is plotted as a function of radius at depths of -11.5 cm and 34 cm, respectively. These depths (see Fig. 1) are measured from the front face of the lead target. The histograms show the calculated values while the plotted points correspond to the experimental measurements. The dashed curve is drawn through the experimental points for comparison purposes. The numerical values in the histogram give the percent standard deviation obtained in the Monte Carlo calculations. The experimental and calculated results are in very good agreement at all radii at both of the depths considered. These comparisons are important from the point of view of shielding because they represent the first definitive test of the ability of the Kinney code using the Bertini data to calculate accurately the low-energy neutrons. Of course the intranuclear-cascade calculations are expected to be more accurate for heavy nuclei such as lead than for light nuclei, so the good agreement in Figs. 2 and 3 cannot be taken to indicate that similar agreement will be obtained with lighter nuclei. Comparisons of calculations with the experimental measurements made using a Be target are in progress but they are not yet available.

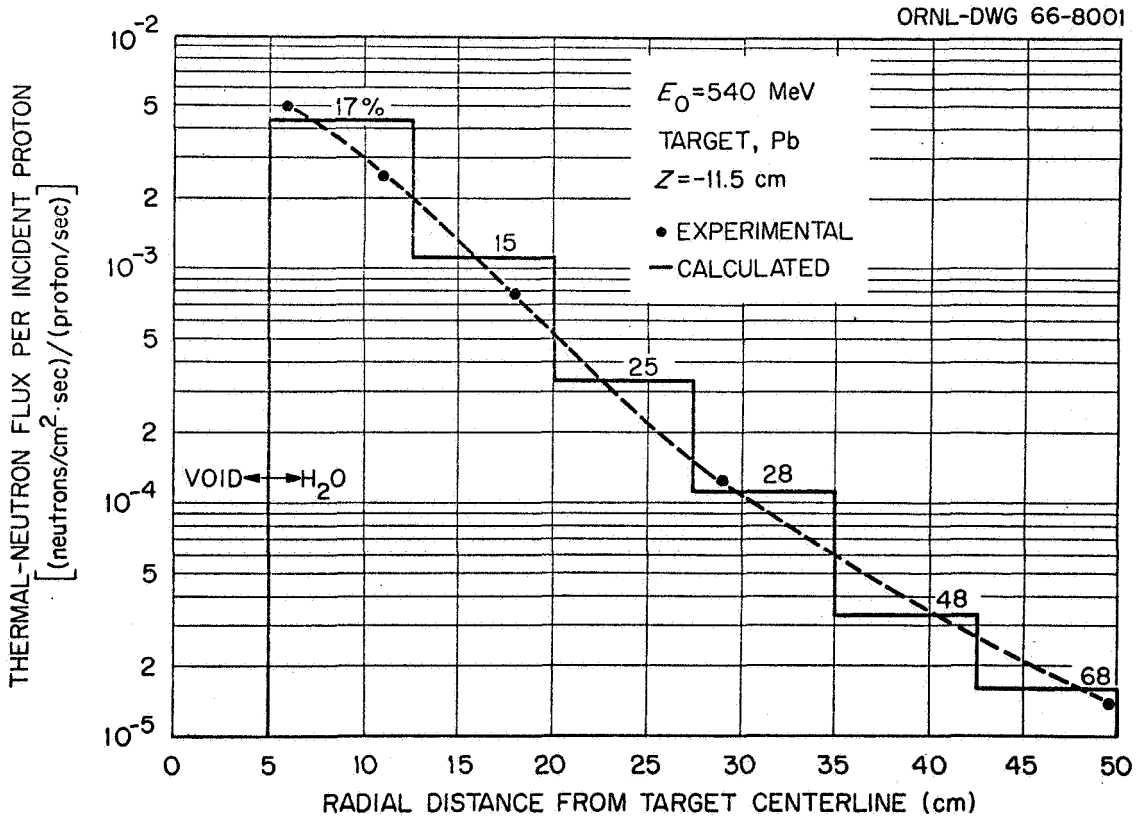
ORNL-DWG 66-8001
THERMAL-NEUTRON FLUX PER INCIDENT PROTON [(neutrons/cm²-sec)/(proton/sec)]
10^{-2}
5
2
10^{-3}
5
2
10^{-4}
5
2
10^{-5}
E_0=540 MeV
TARGET, Pb
Z=-11.5 cm
• EXPERIMENTAL
—CALCULATED
17%
15
25
28
48
68
VOID
H_2O
0
5
10
15
20
25
30
35
40
45
50
RADIAL DISTANCE FROM TARGET CENTERLINE (cm)

Fig. 2.

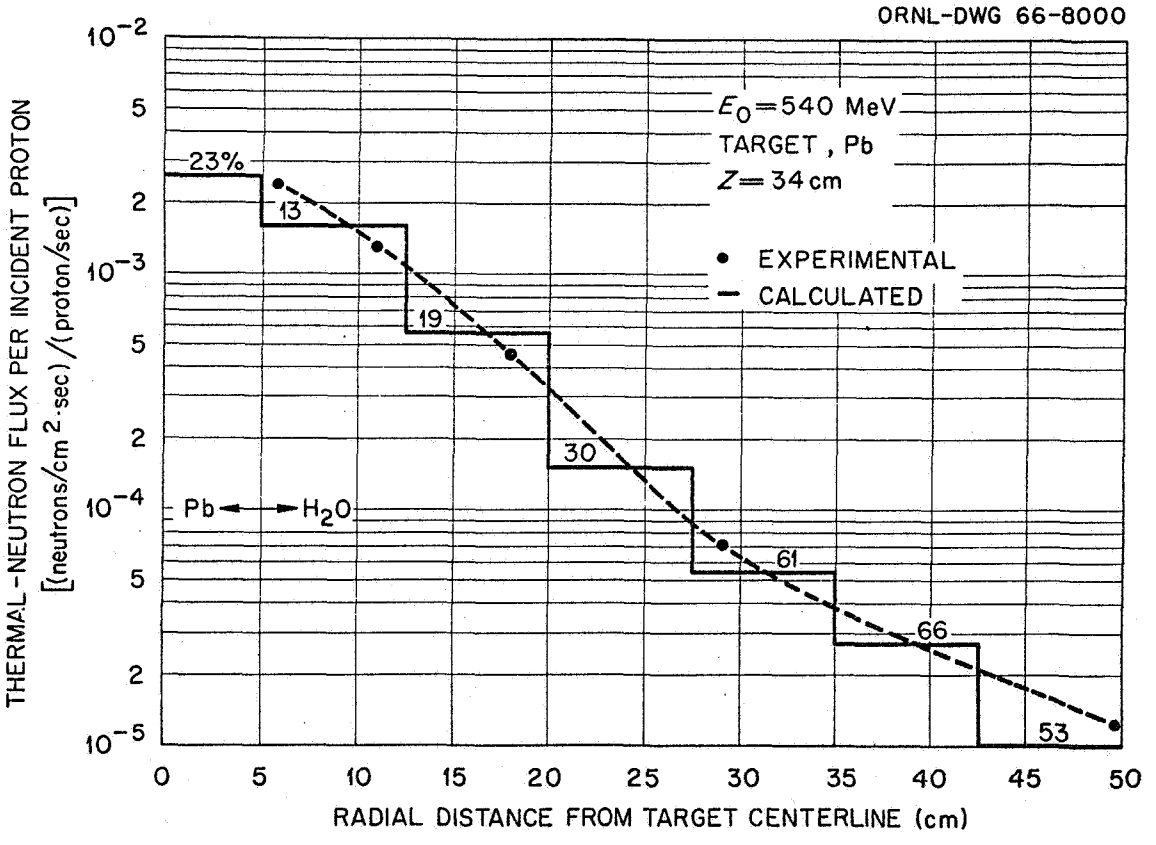
ORNL-DWG 66-8000
E_0=540 MeV
TARGET, Pb
Z=34 cm
EXPERIMENTAL
CALCULATED
23%
13
19
30
61
66
53
Pb
H_2O
THERMAL-NEUTRON FLUX PER INCIDENT PROTON
[(neutrons/cm^2·sec)/(proton/sec)]
RADIAL DISTANCE FROM TARGET CENTERLINE (cm)

Fig. 3.

Comparisons of the calculated and measured particle fluxes emerging from thick targets provide a definitive test of the transport calculations, but such comparisons do not give a very good indication of the error to be associated with calculation of integral quantities such as dose. A series of experimental measurements of the dose as a function of depth in a spherical phantom placed at a variety of positions with respect to a target irradiated by 160-MeV protons has been carried out by T. V. Blosser et al.[7] The geometrical arrangement used in this set of experiments is shown in Fig. 4. For a variety of target materials and thicknesses and for various values of the parameters α, β, θ, and d, the energy deposition, i.e., the dose, was measured as a function of depth in the water phantom. It should be noted that except in the very special case when α, β, and θ are all equal to zero the experimental arrangement is such that the measured dose is due entirely to secondary particles, or, more precisely, to secondary particles and primary particles which have undergone large-angle and multiple small-angle Coulomb scattering.

B. Liley and A. G. Duneer, Jr.[8] have carried out dose calculations and made comparisons with these experimental data. In these calculations which are carried out using Monte Carlo methods, first-generation secondary particles are calculated explicitly and then treated using attenuation factors. The details of the calculations will be published shortly and will not be discussed here. There is, however, one feature of the method employed which I think should be noted. The angular distribution of the first-generation secondary cascade particles is included in the calculations by using an interesting approximation. If $F_{ij}(E',E,\vec{\Omega}'\cdot\vec{\Omega})$ is the number of cascade particles

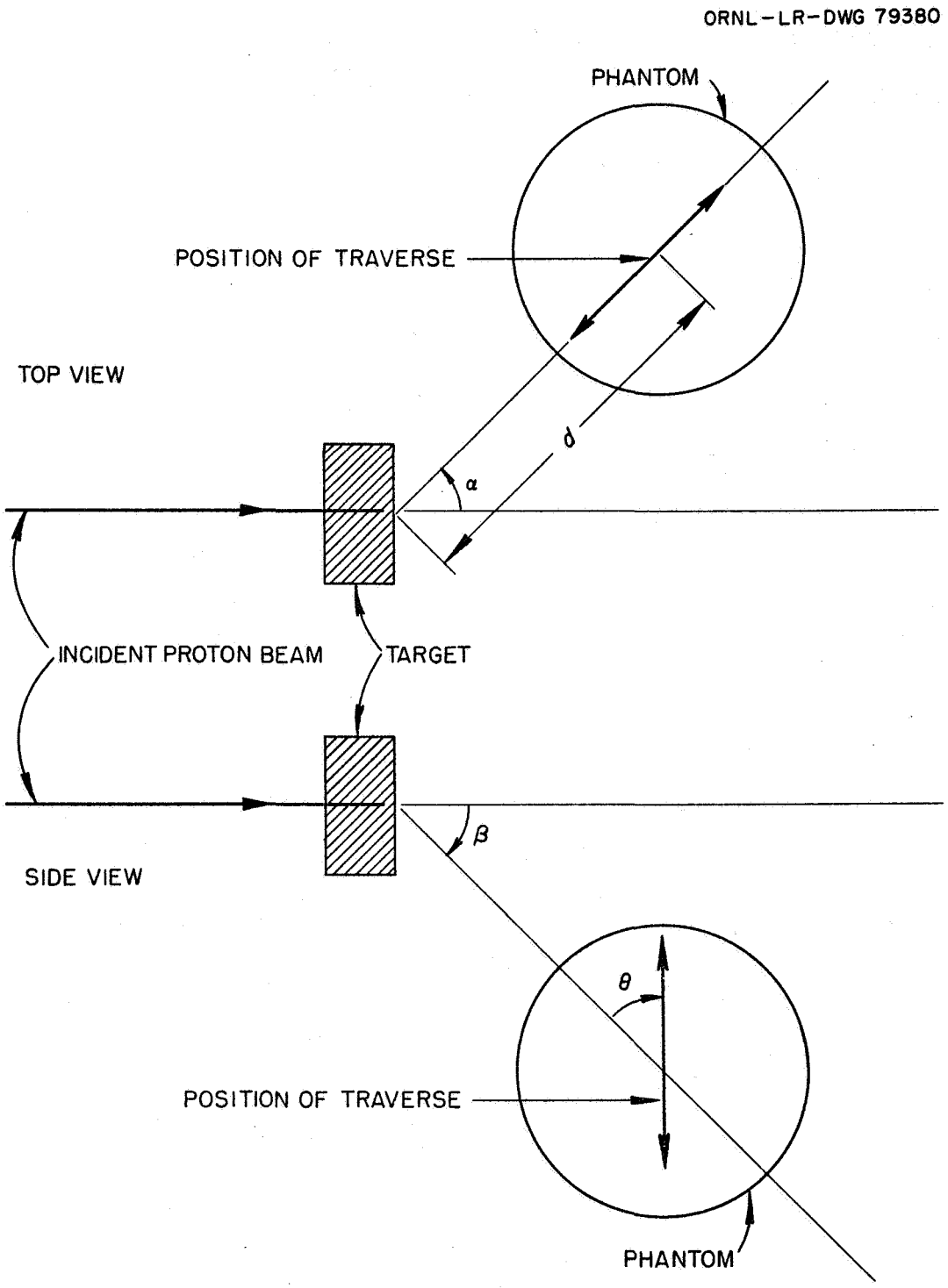
ORNL-LR-DWG 79380
PHANTOM
POSITION OF TRAVERSE
TOP VIEW
d
α
INCIDENT PROTON BEAM
TARGET
β
SIDE VIEW
θ
POSITION OF TRAVERSE
PHANTOM

Fig. 4.

of type i per unit energy about E per unit solid angle about $\vec{\Omega}$ which arises from the nonelastic nuclear collision of a particle of type j with energy E' going in the direction $\vec{\Omega}'$, the assumption is made that

$$F_{ij}(E',E,\vec{\Omega}'\cdot\vec{\Omega}) = f_{ij}(E',E)\, g_{ij}(E',\vec{\Omega}'\cdot\vec{\Omega}) ,$$

where

$$f_{ij}(E',E) = \int_{4\pi} F_{ij}(E',E,\vec{\Omega}'\cdot\vec{\Omega})\, d\Omega$$

$$g_{ij}(E',\vec{\Omega}'\cdot\vec{\Omega}) = \frac{\int_0^{E'} F_{ij}(E',E,\vec{\Omega}'\cdot\vec{\Omega})\, dE}{\int_0^{E'}\int_{4\pi} F_{ij}(E',E,\vec{\Omega}'\cdot\vec{\Omega})\, d\Omega\, dE} ;$$

that is, it is assumed that there is no correlation between the energy of emission and the angle of emission but all of the angular dependence is not omitted. This approximation is interesting because it is in a sense intermediate between using the complete angular dependence and using the often-employed straightahead approximation in which g_{ij} is approximated by $1/2\pi\ \delta(1-\vec{\Omega}'\cdot\vec{\Omega})$. In their calculations Liley and Duneer have used the analytic expressions for g_{ij} obtained by H. Alter.[9] The expressions were obtained by fitting the Monte Carlo data of Bertini[5] by the method of least squares. The angular distribution, g_{PP}, of protons emitted from 150-MeV protons on aluminum obtained by Alter is shown in Fig. 5. In the figure $2\pi\ g_{PP}$ is called SIGMA and MU is used for $\vec{\Omega}'\cdot\vec{\Omega}$. The plotted points show the data obtained from Bertini and the solid curve is the least-square fit. The distribution is peaked forward, but there is, of course, particle emission at angles other than zero.

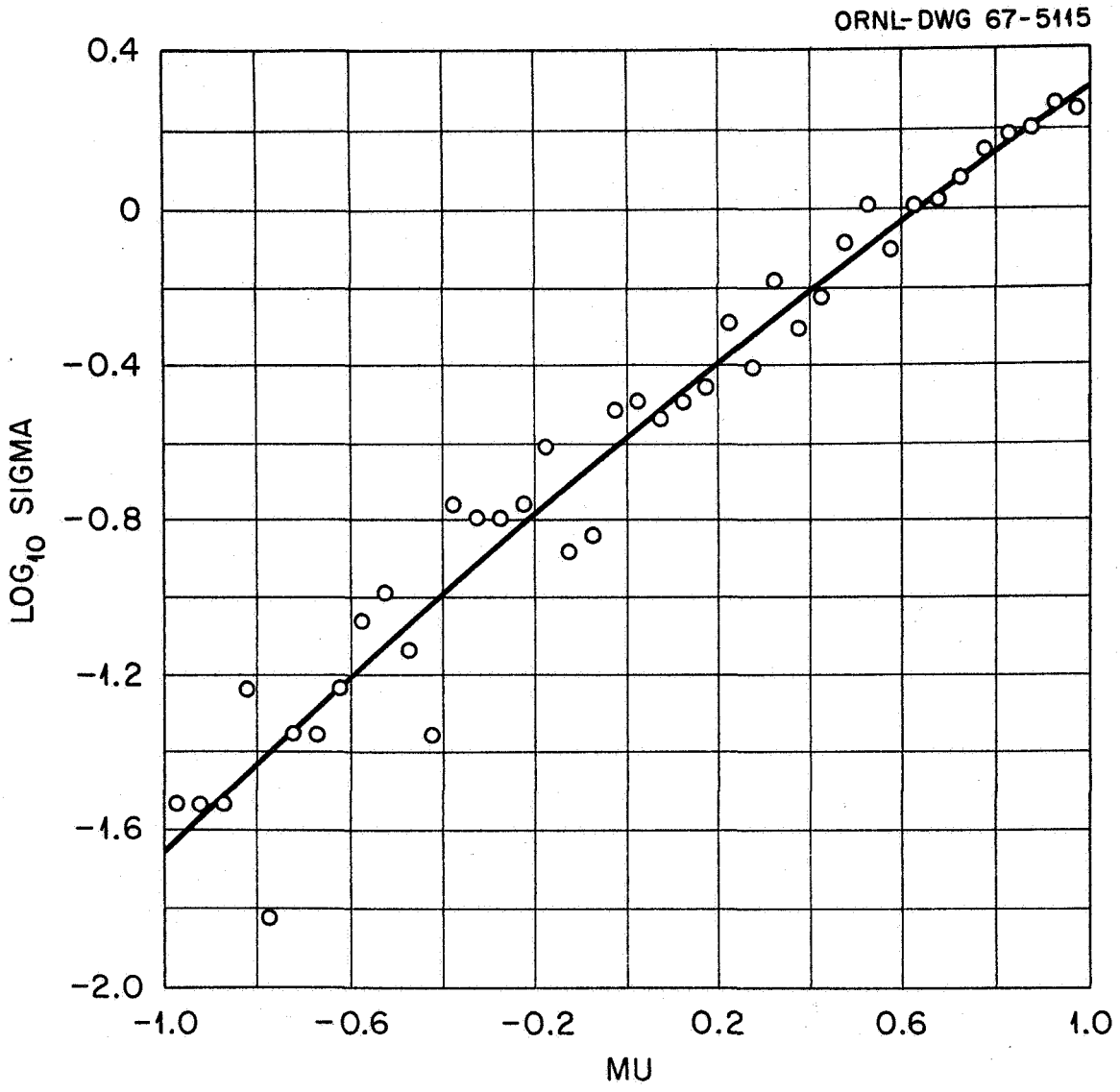

Fig. 5. Cascade Proton Angular Distribution; E = 150 MeV, ^{27}Al.

The comparison between the calculations and the measurements for the case of 160-MeV protons incident on an aluminum target of 26.9 g/cm^2 thickness and $\alpha = \beta = 45^\circ$, $\theta = 0^\circ$, d = 53.7 cm (see Fig. 4) is shown in Fig. 6. The calculations are systematically high compared with the experimental values. In considering this comparison, it must be remembered that the entire contribution to the dose in this case is coming from the secondary particles, and thus the calculational error is not indicative of that which would be obtained in a typical space shielding calculation where the primary particles contribute a large fraction of the dose.

Using Monte Carlo methods, it is feasible to solve the transport equations without approximation. In general, however, to obtain such solutions a large amount of computing time is required, and it is very desirable for design purposes to have methods for obtaining adequate, readily calculable approximate solutions. One such method that is often used employs the straightahead approximation. In this approximation it is assumed that when a nucleon-nucleus collision occurs the secondary particles are emitted in the direction of the incident particle. In a previous paper, the validity of this approximation was tested by comparing exact* calculations with calculations carried out using the approximation for the case of monoenergetic protons isotropically incident on slab shields followed by tissue.[10] A further test of the approximation has now been obtained by making similar comparisons for the case of a typical flare proton spectrum normally incident on a slab shield followed by tissue.[11] For isotropic incidence the angular distribution of the primary particles tends to de-emphasize the angular

*"Exact" is used here to mean calculations in which the angular distribution of the secondary particles is taken into account without approximation. The use of this term is not meant to imply anything about the physical validity of the calculations.

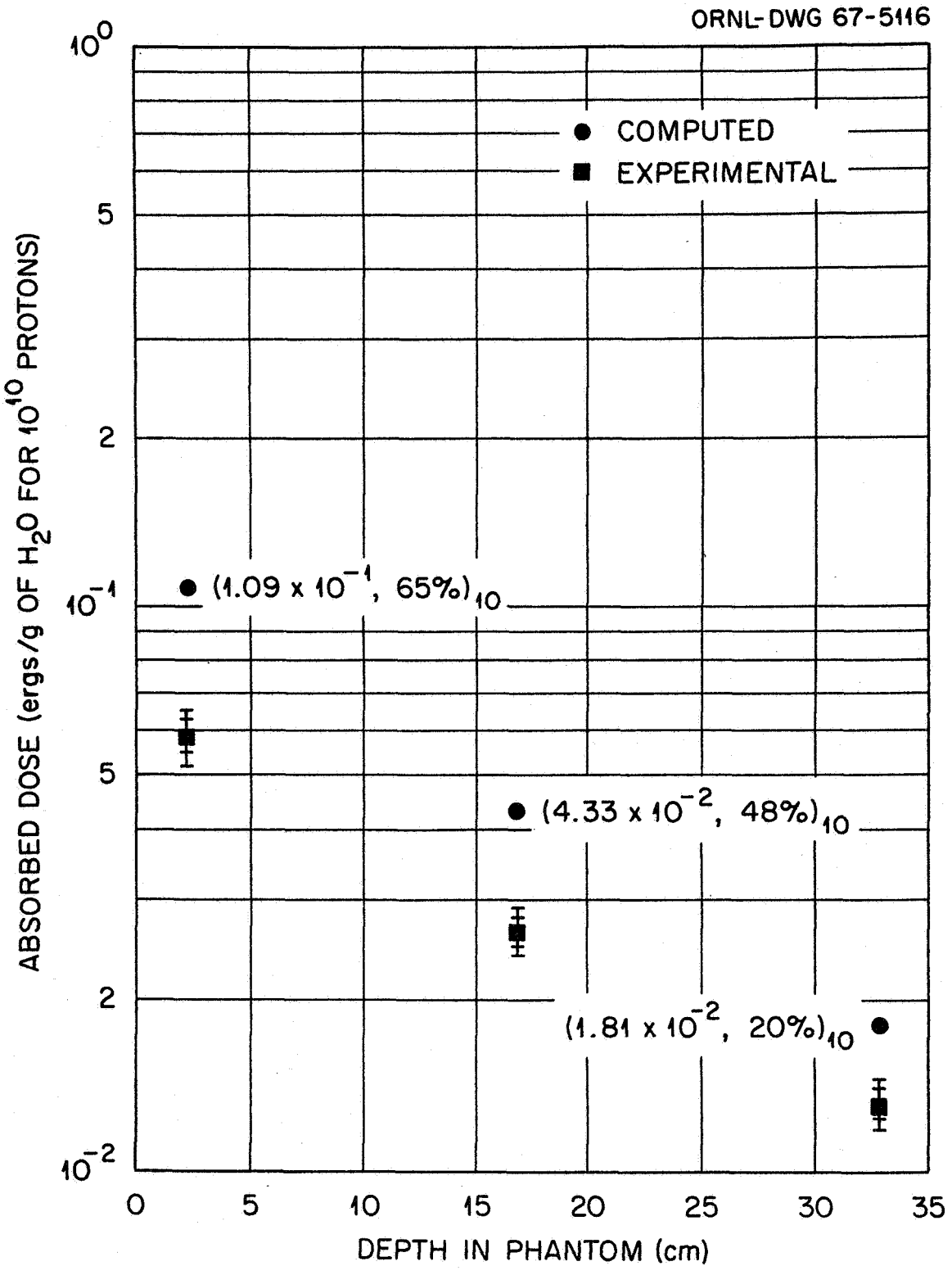
ORNL-DWG 67-5116
COMPUTED
EXPERIMENTAL
(1.09 x 10^-1, 65%)10
(4.33 x 10^-2, 48%)10
(1.81 x 10^-2, 20%)10
ABSORBED DOSE (ergs/g OF H2O FOR 10^10 PROTONS)
DEPTH IN PHANTOM (cm)
10^0
5
2
10^-1
5
2
10^-2
0
5
10
15
20
25
30
35

Fig. 6.

distribution of the secondary particles so the case of normal incidence provides a more stringent test of the approximation than does the case of isotropic incidence.

In order to insure that any differences in the results are due to the approximation being tested and not to such things as differences in nuclear data, both the exact and the straightahead calculations were carried out using the transport code written by W. E. Kinney.[4] The straightahead approximation as used here applies to all particles emitted from nuclear collisions. In both the exact and approximate calculations, the primary protons are assumed to travel in a straight line and continuously lose energy. When a nuclear collision occurs, all of the emitted particles, both evaporation and cascade, are assumed to go in the direction of the incident particle, i.e., no attempt is made to discriminate against particles emitted at large angles as is sometimes done in using the approximation. The flare spectrum used was taken to be exponential in rigidity with a characteristic rigidity of 100 MV and was arbitrarily normalized to 10^9 protons/cm^2 with energy greater than 30 MeV. In the calculations only particles with energy less than 400 MeV were considered. The form of the flare spectrum and the geometry are shown schematically in Fig. 7. The dose calculations in the tissue were carried out as described previously and, in particular, the quality factors used in obtaining the dose in rem are the same as those used previously.[12]

Comparisons between the exact and approximate calculations for the flare spectrum normally incident on 20 g/cm^2 of aluminum (see Fig. 7) are shown in Figs. 8, 9, and 10. In Fig. 8 the exact and approximate secondary proton and neutron currents at the aluminum-tissue interface are compared. The straightahead approximation overestimates the low-energy secondary neutron current and

ORNL-DWG 66-8101

$$J_p(>E) = K\ e^{P(30)/P_0}\ e^{-P(E)/P_0}\ (E < 400\ \text{MeV})$$

$$P(E) = \frac{1}{e}\left[E\,(E+2M_p)\right]^{1/2}$$

$K = 10^9$ protons/cm^2

$P_0 = 100$ MV

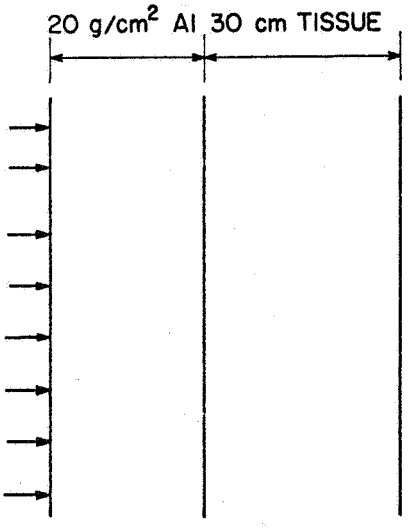

Fig. 7.

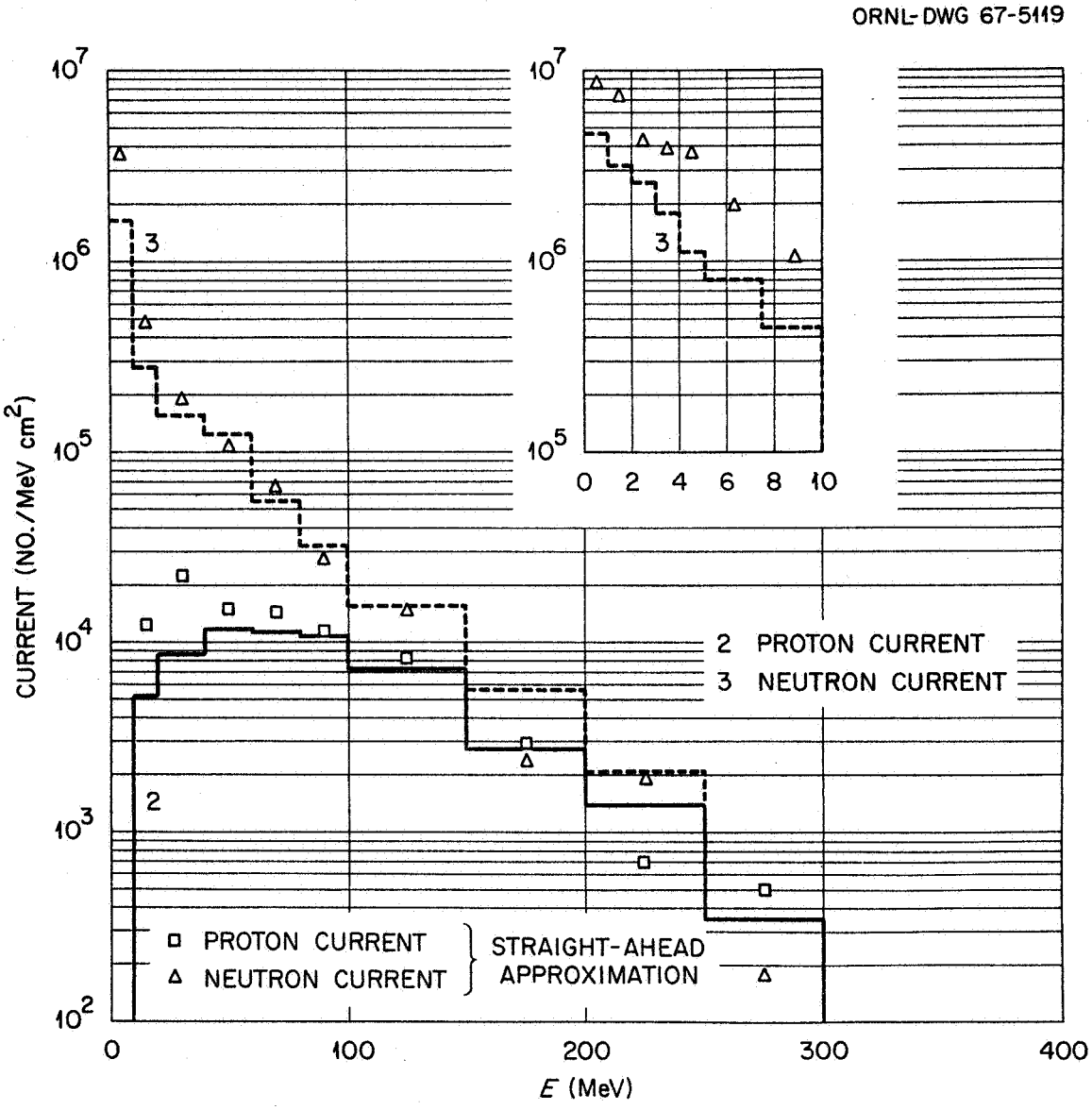

Fig. 8. Secondary Particle Current at Aluminum-Tissue Interface; Flare Spectrum (P_0 = 100 MV) Normally Incident on 20 g/cm^2 of Al Followed by Tissue.

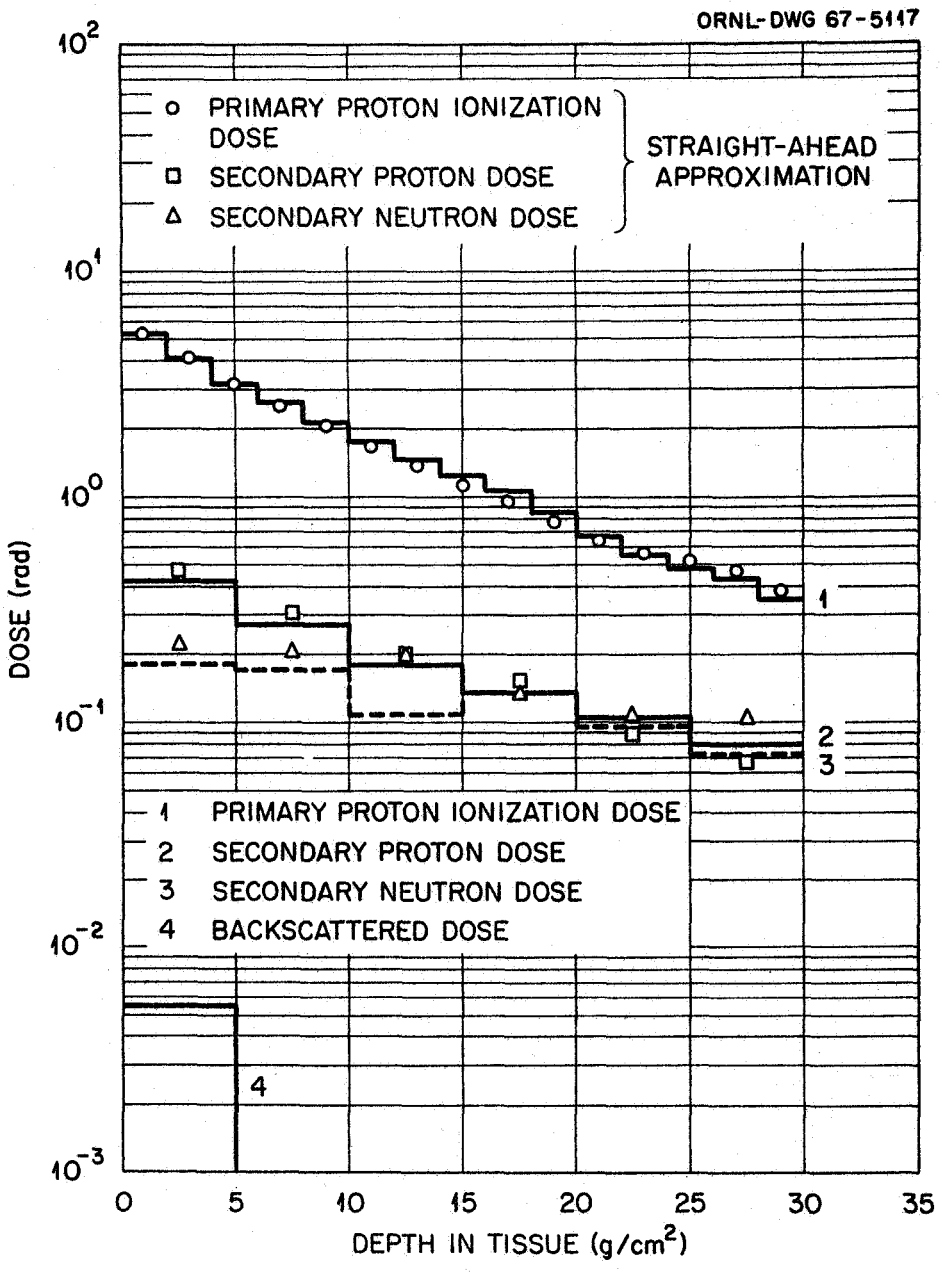

Fig. 9. Tissue Dose (rad) vs Depth; Flare Spectrum (P_0= 100 MV) Normally Incident on 20 g/cm^2 of Al Followed by Tissue.

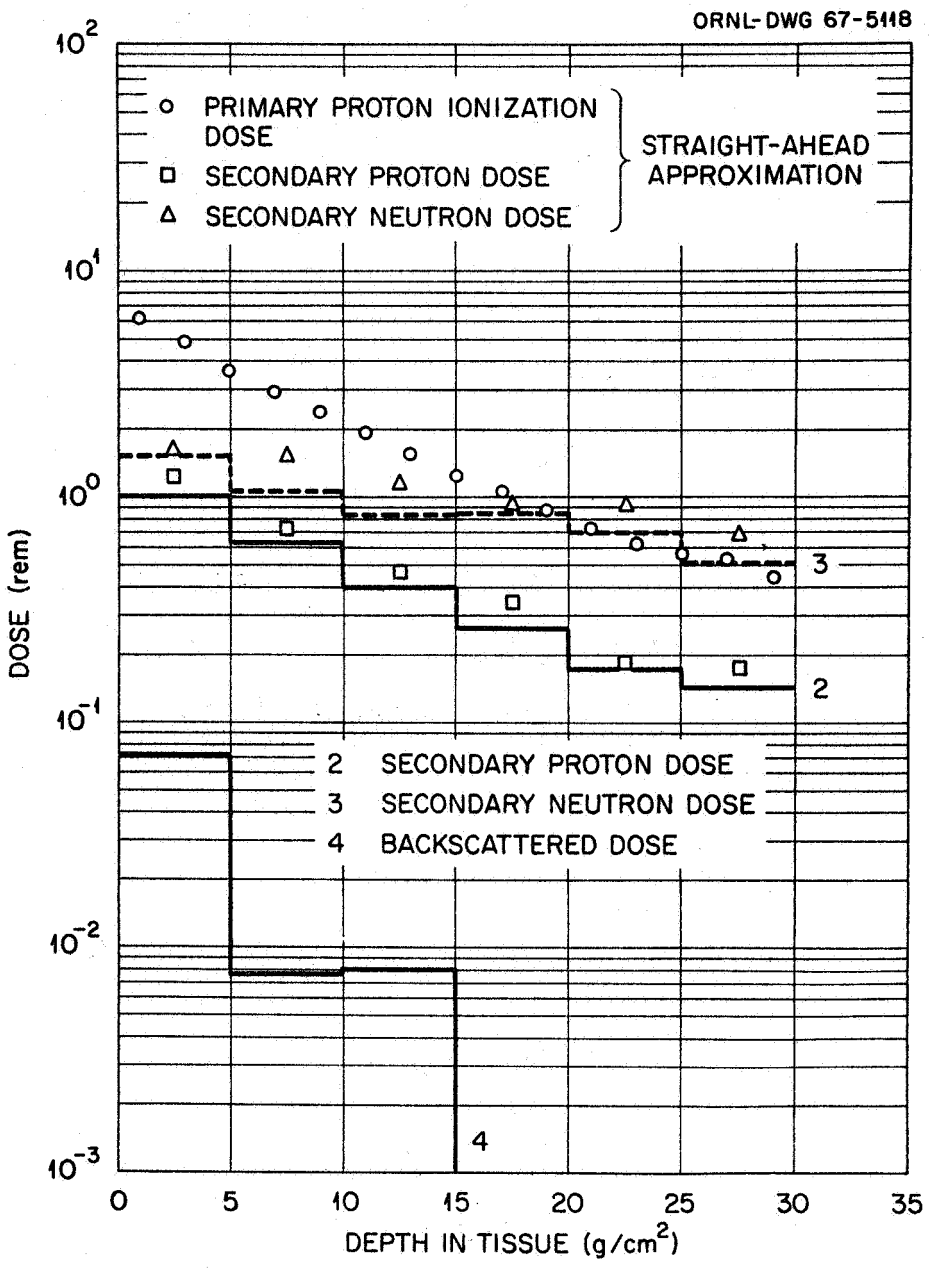

Fig. 10. Tissue Dose (rem) vs Depth; Flare Spectrum (P_0 = 100 MV) Normally incident on 20 g/cm^2 of Al Followed by Tissue.

the low-energy secondary proton current. At high energies (> 100 MeV or so) the statistical fluctuations are large, and the differences between the exact and approximate currents are probably to be ascribed to poor statistics rather than to any failure of the straightahead approximation.

In Figs. 9 and 10 the exact and approximate doses as a function of depth in the tissue in rad and rem, respectively, are shown. For comparison purposes, the total dose has been divided into four parts: primary proton-ionization dose, secondary proton dose, secondary neutron dose, and backscattered dose. The primary proton-ionization dose is the dose from those incident protons which have undergone neither elastic nor nonelastic nuclear collisions. The primary proton-ionization dose is by definition the same in the exact and approximate calculations. Since this is the case, the exact primary proton-ionization dose has not been shown in Fig. 10. The secondary proton dose is the dose from all charged particles that are produced by primary or secondary protons. The secondary neutron dose is the dose from all charged particles produced by secondary neutrons. It should be noted that the secondary proton dose and secondary neutron dose include contributions from particles produced both in the shield and in the tissue. In addition to the contribution from protons, the secondary doses also include a contribution from charged evaporation particles with mass greater than that of a proton and from recoil nuclei. The backscattered dose is the dose from all particles and their progeny which cross from the tissue into the aluminum. This backscattered dose is by definition zero in the straightahead approximation. The agreement between the exact and approximate secondary doses in both Figs. 9 and 10 is quite good at all tissue depths. The straightahead approximation overestimates the secondary doses, particularly in rem, but in the present instance at least the error does not seem excessive from the point of view of shielding. Finally,

it should be noted that while the secondary dose in Fig. 9 is small compared to the primary dose this is not the case in Fig. 10. The quality factors used in the calculations and consequently the dose calculations in rem must be considered to be very approximate. The calculations do serve to indicate, however, that the importance of secondary particles in space vehicle shielding is dependent on the quality factors which are found to be applicable.

At the present time the code collection of the Radiation Shielding Information Center of the Oak Ridge National Laboratory contains five proton penetration codes, written in various approximations, which were designed for doing space shielding calculations. To test the consistency of these codes, W. W. Scott and R. G. Alsmiller, Jr.[13] have compared the results given by each code to a typical sample problem.

The codes which have been considered are those written by W. E. Kinney[4] at the Oak Ridge National Laboratory, by R. P. Moshofsky[14] at The Boeing Company, by C. W. Hill et al.[15] at the Lockheed-Georgia Company, by J. R. Lilley and W. R. Yucker[16]* at the Douglas Aircraft Company, and by R. I. Hildebrand and H. E. Renkel[17] at the Lewis Research Center. An extensive discussion of the data and method of calculation used in each of these codes is given in the listed reference, and therefore only a very brief discussion will be given here. The code written by Kinney is the only one of the codes which solves the complete transport equations. The codes written by Hill et al. and by Hildebrand and Renkel employ the straightahead approximation and include a calculation of the higher generation secondary particles. The codes by Moshofsky and by Lilley and Yucker employ the straightahead approximation, calculate explicitly only

*The code by Lilley and Yucker was not available at the time reference 13 was written and therefore the results from this code presented here are not included in reference 13.

first-generation secondary particles, and utilize attenuation factors to treat the higher generations. The codes by Kinney and by Hildebrand and Renkel use the particle-production data generated by Bertini, while the other codes rely on the older, more approximate data.

The sample problem used in the comparison is that shown in Fig. 7: i.e., a proton flare spectrum, taken to be exponential in rigidity with P_o = 100 MV, normally incident on a slab of aluminum of thickness 20 g/cm^2 followed by a 30-cm slab of tissue. The doses as a function of depth in the tissue from primary protons, secondary protons, and secondary neutrons are compared in Figs. 11, 12, and 13, respectively.

The primary proton doses from the various codes shown in Fig. 11 are in reasonable agreement. This is to be expected since there is little uncertainty in the data, and this dose is relatively easy to calculate. In Fig. 12 where the secondary proton doses are compared, all of the results are in reasonable agreement except those given by the Boeing code.* In Fig. 13 the secondary neutron doses are compared. The Boeing results are somewhat higher than those given by the other codes. The Lockheed-Georgia results appear to be high in the first few centimeters of the tissue but thereafter agree with the results given by the Lewis and Douglas codes. The statistical uncertainty in the ORNL results are rather large, but in general these results are lower than those given by the Lewis and Douglas codes. This difference may be attributed at least to some extent to the straightahead approximation used in the Lewis and Douglas codes.

*M. Wilkinson of Boeing has informed me that he has revised the Boeing code and now obtains results which are in substantial agreement with the other codes. This revised code is not, however, at this time available from the Radiation Shielding Information Center.

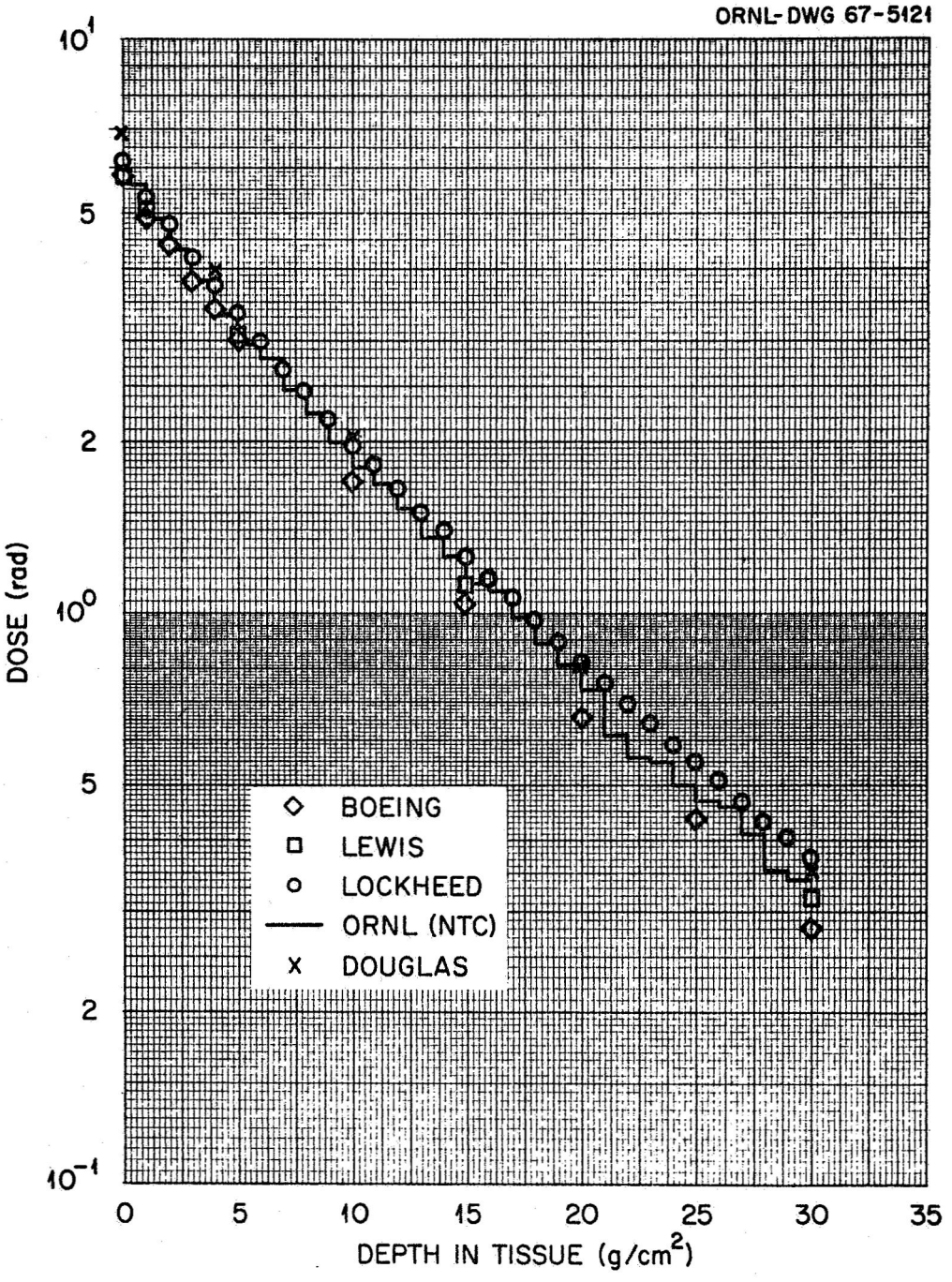

Fig. 11. Primary Proton Dose vs Depth in Tissue.

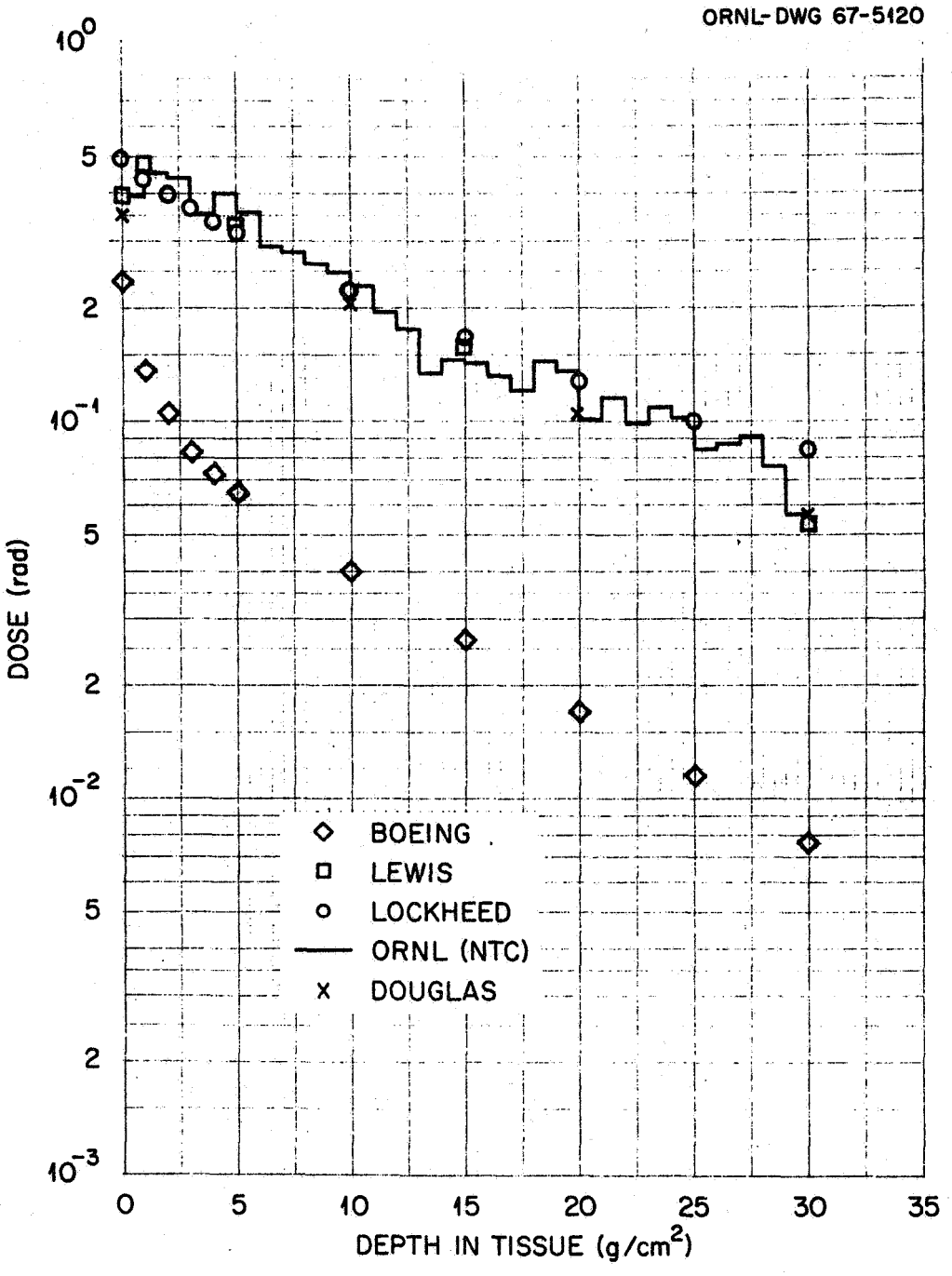

Fig. 12. Secondary Proton Dose vs Depth in Tissue.

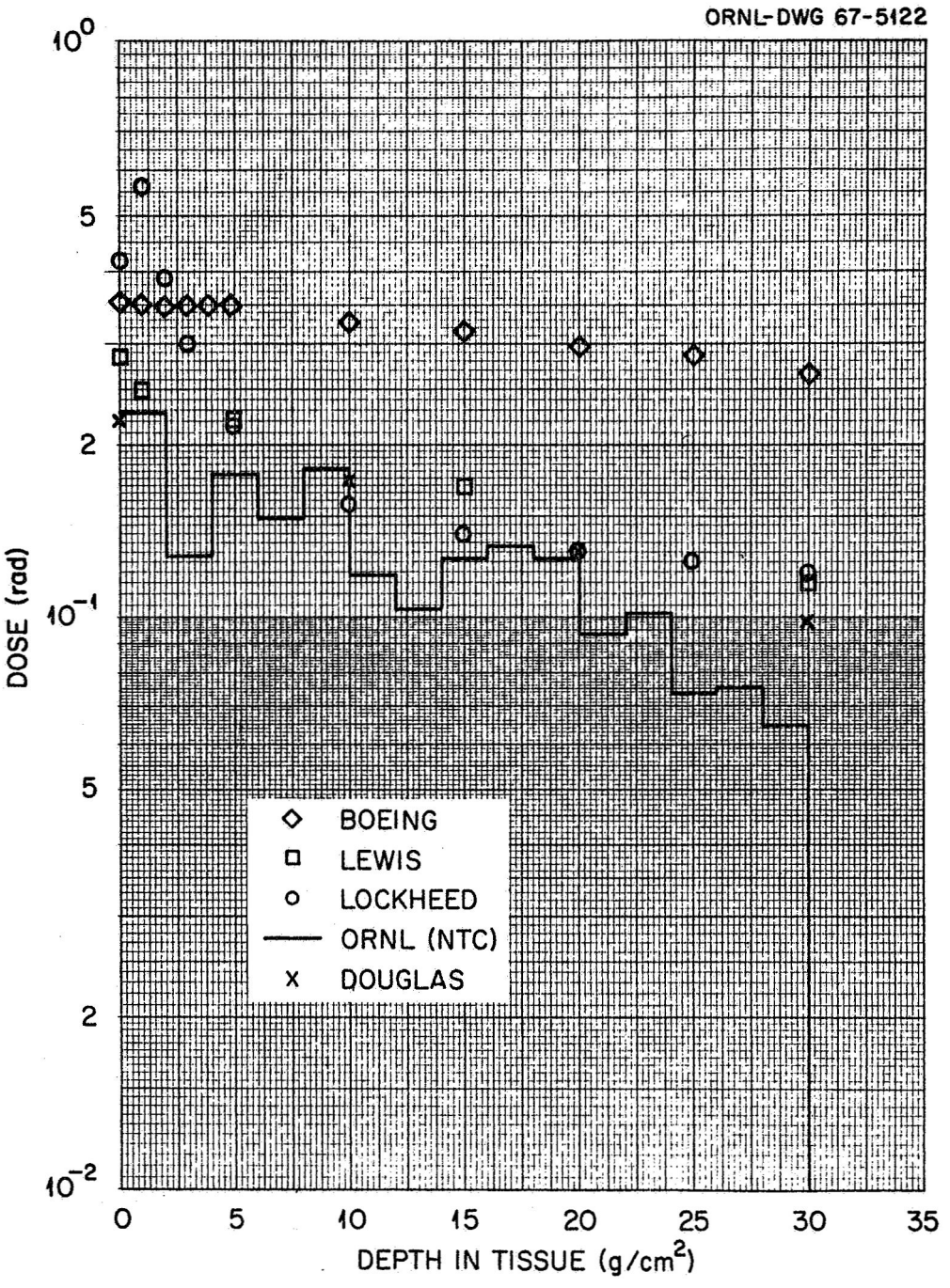

Fig. 13. Secondary Neutron Dose vs Depth in Tissue.

None of the comparisons mentioned above include a contribution from the gamma rays. Calculations have been carried out for gamma rays with the straight-ahead approximation by Madey et al.,[18] Dye,[19] and Alsmiller et al.[20] Gamma-ray calculations have also been performed by Hill et al.,[15,21] who used a model which accounts for the angular distribution of the produced gamma ray and is applicable to a slab shield. In the first three calculations, only gamma-ray production by incident protons was considered; in the last calculation, gamma-ray production by all of the secondary nucleons, as well as the incident protons, is included. Madey et al. and Dye obtained gamma-ray production data by extrapolating from a very limited amount of experimental data. Alsmiller et al. obtained their data by applying crude Coulomb corrections to the theoretical data of Troubetskoy[22] for gamma-ray production by neutrons. These data extended to only 22 MeV. It was assumed that the 22-MeV data applied to protons of energy up to 50 MeV. Hill et al. used the model of Troubetskoy with Coulomb corrections and calculated gamma-emission data at the higher energies.

A comparison of the Madey, Alsmiller, and Hill calculations, due to Hill and Simpson,[21] is shown in Fig. 14. The results shown are the primary proton and gamma-ray doses at the center of a spherical-shell aluminum shield as a function of shield thickness. The form of the incident spectrum considered may be found in Madey et al.[18] and Alsmiller et al.[20] The two Alsmiller curves were obtained using different gamma-ray production data. In obtaining the lower curve, it was assumed that protons with energy greater than 22 MeV could not produce gamma rays; in obtaining the upper curve, gamma-ray production from all protons of energy less than 50 MeV was included. Because of the crude extrapolation used in obtaining the gamma-ray production data, the upper curve is probably an overestimate.

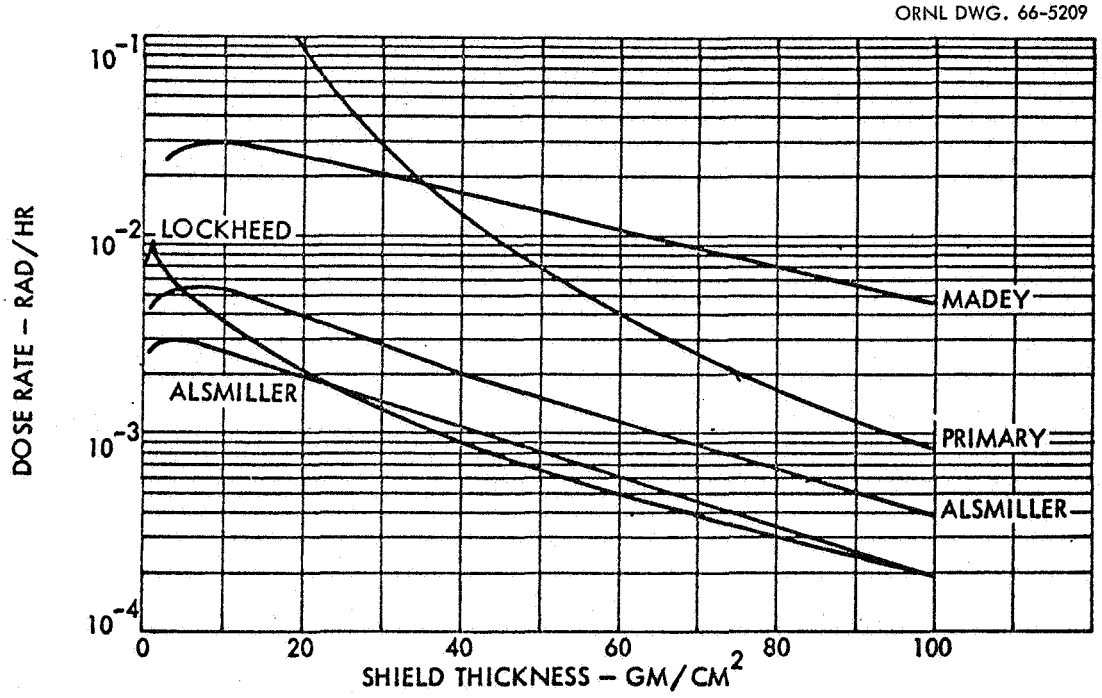

Fig. 14. Primary Proton and Gamma Dose Rate Aluminum Shield.

The Alsmiller et al. and the Hill et al. calculations are in reasonably good agreement except for thin shields. The reason for the thin-shield difference is not known, but probably can be attributed to a difference in the assumed gamma-ray production data for very low energy incident protons. The calculation by Madey et al. is much larger than the other two because of the very different production data used. Experimental information on gamma-ray production from proton-nucleus collisions has recently become available,[23,24] and it is now possible to draw a few tentative conclusions about the validity of the calculations.

In Fig. 15 the interaction cross section multiplied by the number of emitted photons, when a proton collides with an aluminum nucleus, and the interaction cross section multiplied by the total energy of all emitted photons, when a proton collides with an aluminum nucleus, are plotted as a function of incident proton energy. The solid and the dashed curves are obtained from the data used in the calculations of Alsmiller et al., shown in Fig. 14.* If only the solid curves in Fig. 15 are used, then the lower curve labeled Alsmiller in Fig. 14 is obtained. If both the solid and the dashed curves are used, then the upper curve labeled Alsmiller in Fig. 14 is obtained. The plotted points are the experimental points of W. Zobel et al.[23,24] The experimental points have been obtained by integrating the measured differential cross section for photon production and the differential cross section for photon production multiplied by photon energy over all emitted photon energies greater than 600 keV. Hopefully but not certainly the contribution to the integrals from photons of energy less than 600 keV is small.

The upper dashed line in Fig. 15 overestimates considerably the energy emitted in the form of photons multiplied by the cross section between 22 MeV and 50 MeV while the lower dashed line is in very rough agreement with the cross section

*The analogous data used in the calculations of Hill et al. are not given in reference 21, and therefore comparisons with these data cannot be made.

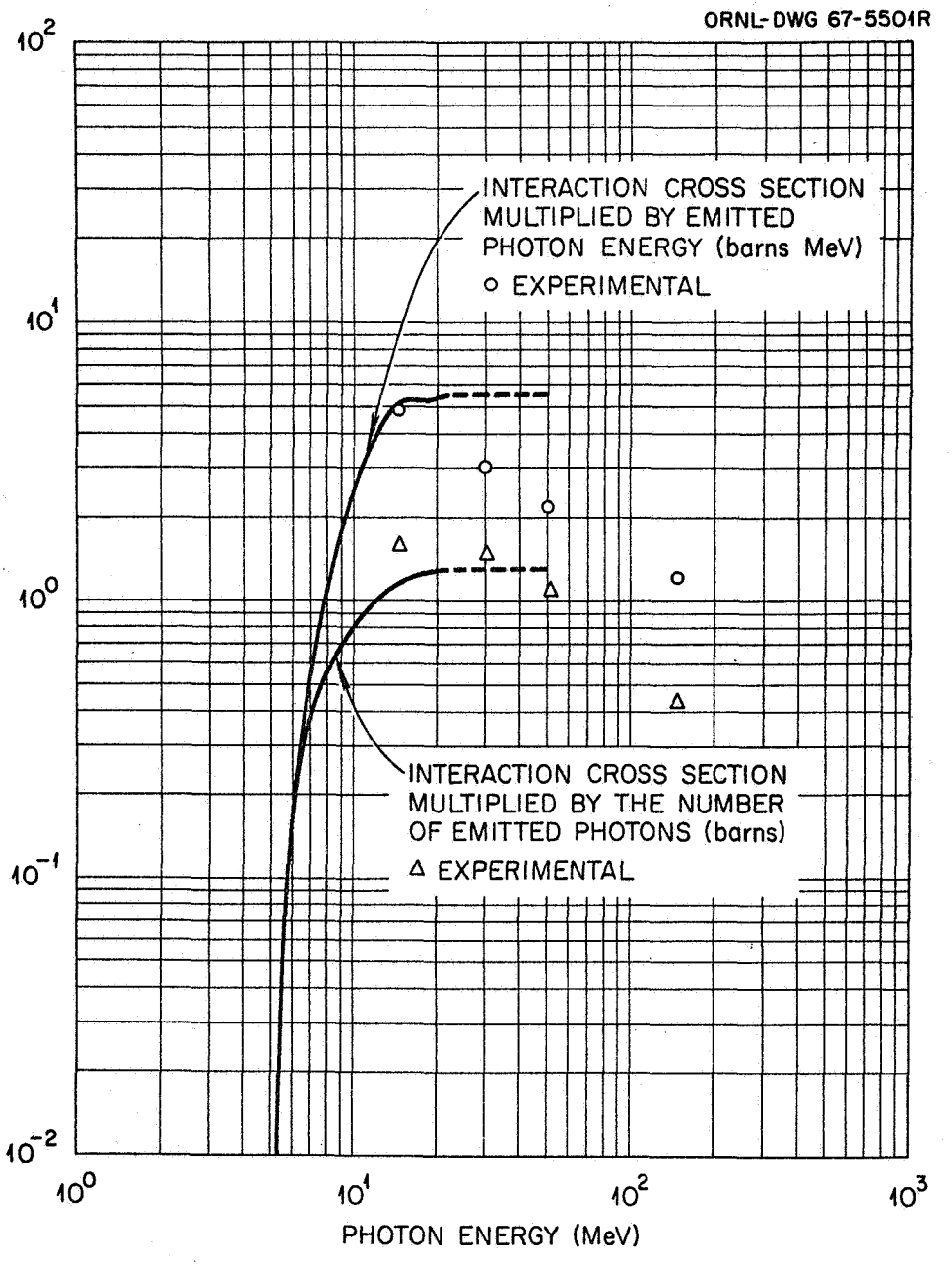

Fig. 15. Photons from Protons Incident on Aluminum.

multiplied by the photon multiplicity in this energy region. This means of course that the upper curve in Fig. 14 labeled Alsmiller is too high. In the energy region from 14.6 MeV to 22 MeV the solid curves underestimate the experimental data on cross section times multiplicity and overestimate slightly the experimental data on emitted photon energy times cross section. On the basis of the comparison shown in Fig. 15, there seems to be no reason to expect that the lower Alsmiller curve in Fig. 14 is greatly in error. Of course the actual photon emission spectrum has not been compared and there may be some changes due to this. Of even more importance, however, is the fact that there are no experimental data for proton energies of less than 14.6 MeV. This energy region is important from the standpoint of gamma-ray production because of the large number of low-energy protons in a typical solar-flare spectrum. If the rapid decrease with decreasing energy of the solid curves in Fig. 15 should be in error, it is still possible that the estimates of the secondary photon contribution to the dose could change appreciably. In this regard, it should also be noted that while secondary nucleon production is a high-energy phenomenon in the sense that the higher energy incident protons ($\geq$ 100 MeV in a typical flare spectrum) tend to be important in their production, this is not the case with secondary gamma rays. All of the calculations, particularly the work of Hill et al.,[21] indicate that the gamma rays produced by very low energy flare protons produce most of the gamma-ray dose even for moderately thick shields. Thus, if the low-energy portion of the flare spectrum, which is not well known, should be much larger than that assumed in the calculations, the gamma dose could increase considerably while the primary proton and secondary nucleon doses remain essentially unchanged.

REFERENCES

1. R. G. ALSMILLER, JR., "High-Energy Nucleon Transport and Space Vehicle Shielding," Nucl. Sci. Eng., 27, 158 (1967).

2. J. S. FRASER et al., "Neutron Production in Thick Targets Bombarded by High-Energy Protons," Phys. Can., 21, No. 2, 17 (1965).

3. W. A. COLEMAN, Oak Ridge National Laboratory, private communication.

4. W. E. KINNEY, "The Nucleon Transport Code, NTC," ORNL-3610, Oak Ridge National Laboratory (1964).

5. H. W. BERTINI, "Low-Energy Intranuclear-Cascade Calculations," Phys. Rev. 131, 180 (1963); with erratum, Phys. Rev., 138, AB2 (1965).

6. L. DRESNER, "EVAP - A FORTRAN Program for Calculating the Evaporation of Various Particles from Excited Compound Nuclei," ORNL-TM-196, Oak Ridge National Laboratory (1961).

7. T. V. BLOSSER, F. C. MAIENSCHEIN, and R. M. FREESTONE, JR., "The Energy Deposition in a Water-Filled Spherical Phantom by Secondaries from High-Energy Protons and by Neutrons," Health Phys., 10, 743 (1964).

8. B. LILEY and A. G. DUNEER, JR., "Secondary-Dose Equivalent Model and Comparison of 160-MeV Proton-Induced Neutron and Proton Dose with a Comprehensive Experiment," Space and Information Systems Division, North American Aviation, Inc. (submitted to Nuclear Science and Engineering).

9. H. ALTER, "Basic Microscopic Data for Space Shielding Analysis," AI-Memo-8853, Atomics International, North American Aviation, Inc. (1963).

10. R. G. ALSMILLER, JR., D. C. IRVING, and H. S. MORAN, "The Validity of the Straightahead Approximation in Space Vehicle Shielding Studies," Second Symposium on Protection Against Radiations in Space, Gatlinburg, Tenn., Oct. 12-14, 1964, NASA SP-71, p. 177, National Aeronautics and Space Administration (1965).

11. This work was carried out by R. G. ALSMILLER, JR., D. C. IRVING, and H. S. MORAN at the Oak Ridge National Laboratory.

12. C. D. ZERBY and W. E. KINNEY, "Calculated Tissue Current-to-Dose Conversion Factors for Nucleons Below 400 MeV," Nucl. Instr. Meth., 36, 125 (1965).

13. W. W. SCOTT and R. G. ALSMILLER, JR., "Comparison of Results Obtained with Several Proton Penetration Codes," RSIC-17, Oak Ridge National Laboratory (1967).

14. R. P. MOSHOFSKY, "Computer Codes for the Evaluation of Space Radiation Hazards. Vol. 8: Space Radiation Doses from Protons and their Secondary Radiations," D2-90418-8 (NASA-CR-58299), Aerospace Div., The Boeing Company (1964).

15. C. W. HILL et al., "Computer Programs for Shielding Problems in Manned Space Vehicles," ER-6643 (NASA Contract NAS8-5180), The Lockheed-Georgia Company (1964).

16. J. R. LILLEY and W. R. YUCKER, "Charge, A Space Radiation Shielding Code," SM-46335, Douglas Missile and Space Systems Division, Douglas Aircraft Company (1965).

17. R. I. HILDEBRAND and H. E. RENKEL, "The Lewis Proton Shielding Code," NASA TM X-52166, Lewis Research Center (1966).

18. R. MADEY et al., "Gamma Dose from Solar Flare Protons Incident on an Aluminum Shield," Trans. Am. Nucl. Soc., 5, 1, 213 (1962).

19. D. L. DYE, "Space Proton Dose at Points Within the Human Body," DZ-90106, The Boeing Company (1962).

20. F. S. ALSMILLER, R. G. ALSMILLER, JR., and D. K. TRUBEY, "Comparison of Primary Proton Dose with the Dose from Gamma Rays Produced by Inelastic Scattering of Solar Flare Protons," Proc. Symposium on Protection Against Radiation Hazards in Space, Gatlinburg, Tenn., Nov. 5-7, 1962, TID-7652, Division of Technical Information Extension, USAEC (1962).

21. C. W. HILL and K. M. SIMPSON, JR., "Calculation of Proton Induced Gamma-Ray Spectrum and Comparison with Experiment," Proc. Second Symposium on Protection Against Radiations in Space, Gatlinburg, Tenn., Oct. 12-14, 1964, NASA SP-71, p. 189, National Aeronautics and Space Administration (1965).

22. E. S. TROUBETSKOY, "Fast Neutron Cross Sections of Iron, Silicon, Aluminum, and Oxygen," NDA-2111-3, Vol. C, Nuclear Development Associates, Inc. (1959).

23. W. ZOBEL, F. C. MAIENSCHEIN, and R. J. SCROGGS, "Spectra of Gamma Rays Produced by the Interaction of ~160-MeV Protons with Be, C, O, Al, Co, and Bi," ORNL-3506, Oak Ridge National Laboratory (1965).

24. W. ZOBEL, Oak Ridge National Laboratory, private communication.

Internal Distribution

1-3. L. S. Abbott
4. F. S. Alsmiller
5-30. R. G. Alsmiller, Jr.
31. T. W. Armstrong
32. H. W. Bertini
33. F. E. Bertrand
34. W. R. Burrus
35. C. E. Clifford
36. W. A. Gibson
37. M. P. Guthrie
38. D. C. Irving
39. W. H. Jordan
40. T. A. Love
41. F. C. Maienschein
42. R. W. Peelle
43. R. T. Santoro
44. D. K. Trubey
45. J. W. Wachter
46. A. M. Weinberg
47. W. Zobel
48. G. Dessauer (consultant)
49. B. C. Diven (consultant)
50. M. H. Kalos (consultant)
51. L. V. Spencer
52-53. Central Research Library
54. Document Reference Section
55-285. Laboratory Records Department
286. Laboratory Records ORNL RC
287. ORNL Patent Office

External Distribution

288. James E. McLaughlin, Director, Radiation Physics Division, U. S. Atomic Energy Commission, Health and Safety Laboratory, 376 Hudson Street, New York, New York 10014
289. P. B. Hemmig, Division of Reactor Development and Technology, U. S. Atomic Energy Commission, Washington, D. C. 20545
290. I. F. Zartman, Division of Reactor Development, U. S. Atomic Energy Commission, Washington, D. C. 20545
291-304. Division of Technical Information Extension (DTIE)
305. Division of Research and Development (ORO)